ORBITING TRANSMISSION SOURCE FOR POSITRON TOMOGRAPHY*

R.H. Huesman, S.E. Derenzo, J.L. Cahoon, A.B. Geyer,
W.W. Moses, D.C. Uber, T. Vuletich, and T.F. Budinger

Donner Laboratory and Lawrence Berkeley Laboratory
University of California
Berkeley, CA 94720

November 12, 1987

Abstract

Accidental suppression and effective data rates have been measured for the orbiting transmission source as implemented in the Donner 600-Crystal Positron Tomograph. A mechanical description of the orbiting source and a description of the electronics used to discard scattered and accidental events is included. Since accidental coincidences were the rate-limiting factor in transmission data acquisition, the new method allows us to acquire sufficient transmission data in a shorter time with a more active transmission source.

Introduction

Quantitative positron emission tomographic imaging requires correction for the attenuation of annihilation photons that are emitted from sources in the patient. Correction for this attenuation can be accomplished by analytical methods if the distribution of scattering medium is known or can be accurately approximated, but a more accurate technique involves direct measurement of the attenuation using annihilation photons from an external positron source.[1] This paper describes an orbiting transmission source used by the Donner 600-Crystal Positron Tomograph to estimate the photon attenuation due to the presence of the patient. Particular attention is given to the methods used to reject spurious data due to accidental coincidences and Compton scattering within the patient.

The data used to compute the attenuation correction factors are acquired while a positron emitting source traverses an integral number of circular orbits around the longitudinal axis, within the shielding gap of the tomograph. The number of counts for each crystal-crystal combination (chord) is measured with the patient in and out of the tomograph, and the quotient (chord by chord) of these two datasets is the fractional data loss as a function of position and angle of chords in the transverse section. These chord-by-chord attenuation factors are used to correct emission datasets for attenuation. We refer to the data acquired with the patient in the tomograph as the "transmission" dataset, and the data acquired with the tomograph empty as the "efficiency" dataset. (The efficiency dataset can also be used to estimate crystal-pair efficiency corrections.) Two primary sources of spurious events that lead to errors in the attenuation correction which are minimized with this modality are: accidental coincidences (those resulting from two separate positron annihilations) and scatter events (annihilations where at least one of the photons Compton scatters in the patient, but is still detected by the tomograph).

The method of using an orbiting transmission source to measure the attenuation correction was first proposed in 1981.[2] It has since been incorporated into several commercial positron tomographs, the first of which was the Cyclotron Corporation Model 4600 Neuro-Tomograph.[3] Increased contrast in transmission images which arises from the scatter rejection of this modality has also been reported.[4] The implementation discussed here is part of the Donner 600-Crystal Positron Tomograph[5], which is equipped with an orbiting source and is able to acquire transmission and efficiency data at a rate of over one million events per second.

The implementation discussed in this paper differs from other systems in the manner in which accidental coincidences and scattered data are rejected. By accepting only those events consistent with emanations from the orbiting transmission source, both accidental coincidences and scattered data are dramatically reduced and a better estimate of attenuation factors is obtained. This rejection of spurious events is especially important when the transmission datasets are acquired at the high data rates needed to make the scans short enough to accommodate reasonable patient comfort, as the fraction of accidental coincidences rises rapidly with increasing count rate.

In this study we analyze rejection of the accidental coincidences. A study of the rejection of scattered data is in progress.

*This work was supported in part by the U.S. Department of Energy, under Contract No. DE-AC03-76SF00098, and in part by Public Health Service Grant Nos. P01 HL25840 and R01 CA38086.

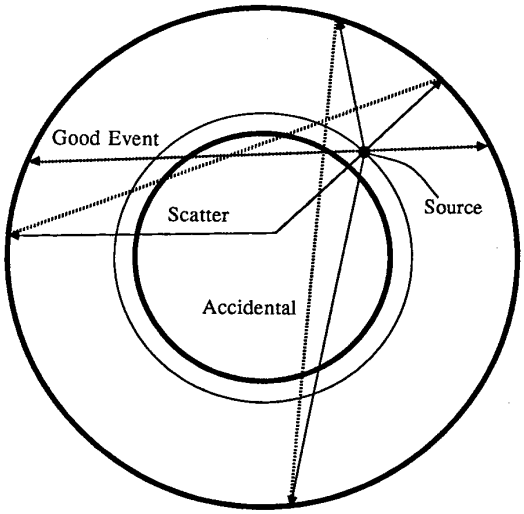

Figure 1: The orbiting transmission source

Methods

Theory

Figure 1 shows the geometry of a circular positron tomograph with an orbiting transmission source. The outer dark circle represents the position of the ring of photon detectors, and the inner dark circle represents the patient port. The large dot represents the orbiting source, and the light circle represents its orbit. Since this positron source is in the shape of a rod perpendicular to the transverse section, it appears as a small point in the tomographic slice.

Also shown in figure 1 are three types of events: good events (unscattered, from the same positron), scattered events (from the same positron), and accidental events (two photons from different positrons). A chord is assigned to an event by the points of detection of the photons, and the shaded lines represent these chords. Note that while the chord from a good event passes through the orbiting source, the chords from scattered and accidental events do not. Since the position of the orbiting source is known, the scattered and accidental events whose chords do not pass through the source can be rejected.

Rejection of the events whose chords do not pass reasonably close to the orbiting source is performed with the data acquisition electronics of the Donner 600-Crystal Positron Tomograph with the following algorithm. Figure 2 shows a representation of acquired data with the source stationary. This representation of the data, organized by transverse chord position (horizontal) and chord angle (vertical), is called a "sinogram".[6] The data from good events (the dark line in figure 2) form a sine wave in the vertical direction, while the data from scatter and accidental events populate the two-dimensional space more uniformly. Therefore, a mask is placed around the sine wave describing the predicted positions on the sinogram of the good events and is stored in memory. This mask, represented by the light lines on either side of the dark sine wave, is then used to test whether an event should be rejected because the corresponding chord does not pass through the source.

As the source moves in its circular orbit, this sine wave pattern moves in the vertical direction, so the appropriate mask for an arbitrary source position can be generated by a vertical shift of a single mask. This vertical translation is performed by replicating the mask several times in memory and then adding to the sinogram address of the event in question an offset which corresponds to the position of the rotating transmission source.

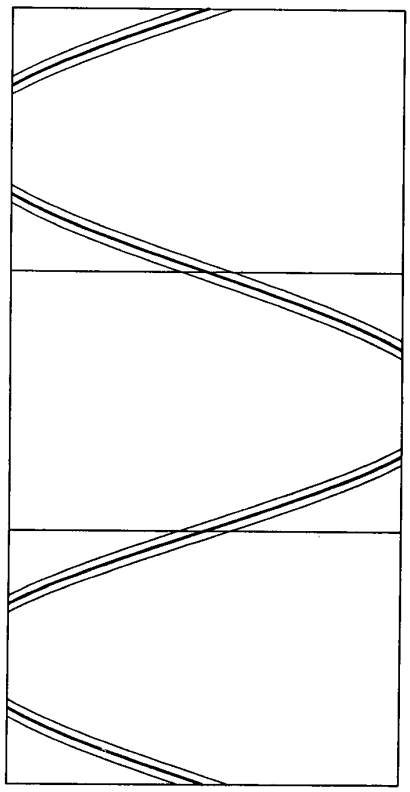

Figure 2: Sinogram and rotating mask for orbiting transmission source: memory address = histogram address + source position offset. The source position offset is changed as the source traverses its orbit.

The offset changes by 201 (the number of projection bins in one of 300 discrete angles) as the source passes from the front of one crystal to the front of the next. In order to accommodate the 360° orbit of the transmission source, three copies of the mask are needed in the memory. Notice that in the central area the mask has been flipped in the horizontal direction.

Mechanical Description

Figure 3 schematically shows the mechanical arrangement of the orbiting transmission source. The 600 detectors of the tomograph are close-packed in a circle with a radius of 30 cm; the

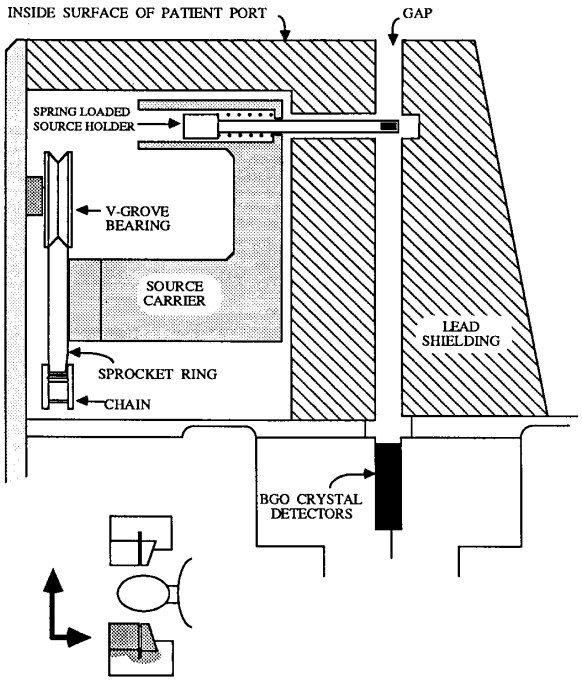

Figure 3: Mechanical schematic of the orbiting transmission source

patient port has a radius of 15 cm, and the orbit of the source has a radius of 17.8 cm. The orbiting source is a 5 mm diameter by 3 mm long ^{68}Ge cylinder, encapsulated in the tip of a stainless steel rod, that can be deployed and rotated inside the lead shielding gap, and in front of the crystal detectors. The stainless steel rod can be attached to, and removed from, a sprocket ring. The sprocket ring is driven by a stepping motor via a chain, and rides on six V-groove ball bearings that keep its axis of rotation concentric with the ring of photon detectors. The position of the source is determined by an indexing pulse generated by a stationary micro-switch and a cam lobe mounted on the sprocket ring. The exact position is determined by counting the number of step commands sent to the stepping motor since the last index pulse. The sprocket ring makes one revolution for 2400 step commands (four steps between detectors).

When the source is not being used, it is parked inside the lead shielding of the tomograph. The source is deployed by driving the sprocket ring to a "load" position, where a solenoid driven arm pushes the source into a latching mechanism that holds the source firmly to the sprocket ring. After the solenoid arm retracts, the source and sprocket assembly can be rotated as a single unit. The source is removed by driving the sprocket ring to an "unload" position, where the solenoid arm activates a release trigger, and the source is driven into its housing by a spring.

Electronics

Figure 4 is a block diagram of the electronics that controls the masking operation. A Motorola MC6809 microprocessor con-

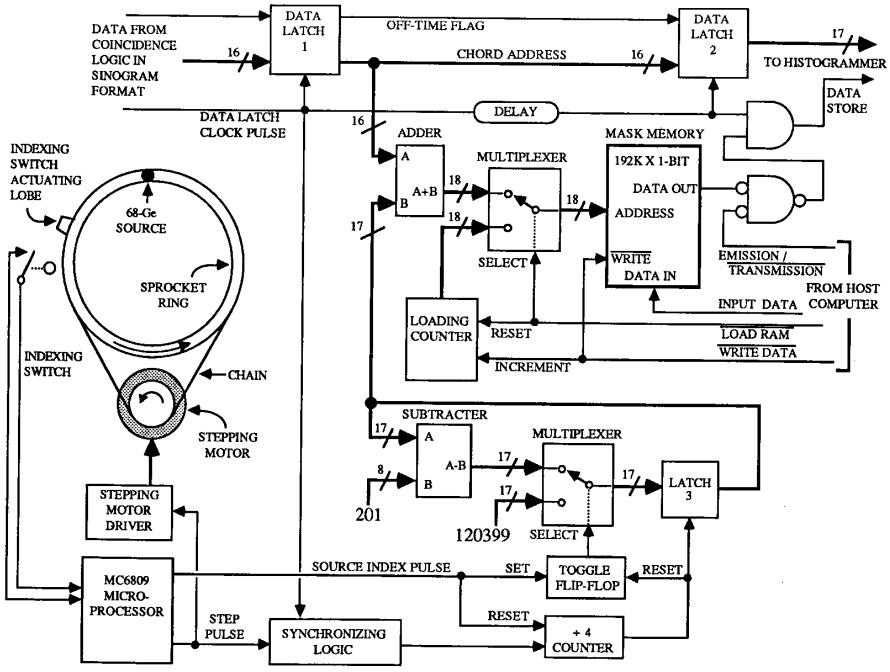

Figure 4: Block diagram of the electronics for rejection of events using a mask located in memory

trols stepping motor ramping and step rate, source position determination and indexing, source loading and unloading, and some of the data acquisition functions. Synchronizing logic is provided to guarantee that input data and step commands are not lost when they occur simultaneously.

The masking described above is performed as follows. A sinogram mask corresponding to a single source position is generated on the host computer and loaded into a 192K by 1-bit look-up memory. Since the proper mask for an arbitrary source position can be generated by a vertical shift of this sinogram mask a number determined by the position of the source is added to the sinogram address of the chord in question. If the mask bit at this combined address is set, corresponding to the chord passing through the source, then the event is sent on to be histogrammed.

The number determined by the position of the source is generated by a multiplier circuit whose output is the product of the source position and the constant 201, the number of projection bins in each angle of the sinogram. In this case, multiplication is performed by repeatedly subtracting 201 from a starting constant every time the stepping motor has moved four steps. The starting constant (120399) is the product of 201 projection bins times the number of photon detectors. The number representing the detector count is 599, instead of 600, since the circuitry uses zero as a valid detector number. Therefore, the source position number that is sent to the adder starts at 120399 and decrements to zero (end of a complete rotation) in intervals of 201.

The process is initialized on every full rotation of the sprocket ring. A source index pulse, generated by the microprocessor, sets a toggle flip-flop that causes a multiplexer to select and route the starting constant to the input of an edge-triggered latch (latch 3 in figure 4). At this point, the data on the output of the latch is zero, assuming that at least one index pulse has previously been generated, and the addresses sent to the mask memory from the adder are just the chord addresses.

The step command immediately following a source index pulse causes the divide-by-four counter to generate a signal edge that resets the toggle flip-flop until the next index pulse. The multiplexer then routes the output of the subtracter (the starting constant minus 201) to the input of the latch. At the same time, the starting constant is transferred to the output of the latch, and addresses sent to the mask memory are the chord addresses plus 120399.

Effective data rate

An "off-time" window is used to correct for accidental coincidences on the Donner 600-Crystal Positron Tomograph.[7] For off-time events, histogram data are decremented instead of incremented, so that correction for accidentals is performed during the data acquisition. The rate of accumulation of events in the histogrammers is therefore given by $R_o - R_f$, where R_o and R_f are the data rates for on-time and off-time events, respectively.

We define the effective data rate for this method of data acquisition as,

$$R_{eff} = \frac{(R_o - R_f)^2}{R_o + R_f} . \qquad (1)$$

This effective data rate, R_{eff}, is less than R_o when the data rate is high enough to produce a significant fraction of accidental coincidences. R_{eff} can be interpreted as the data rate necessary to obtain a dataset of comparable statistical quality in the same time if the phenomenon of accidental coincidences did not exist.

The effective date rate is the figure of merit we will use to compare the quality of data acquired with different levels of source activity and different masks.

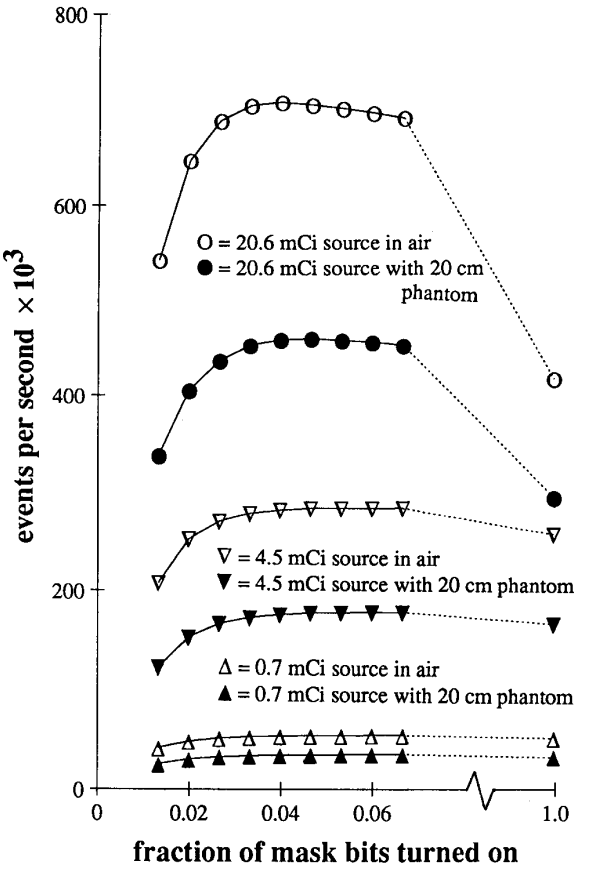

Figure 5: Effective data rate as a function of mask size, source strength, and attenuating distribution. Points at the right are for all mask bits off (no masking).

Results

Data were acquired for three orbiting source strengths: 0.7 mCi, 4.5 mCi, and 20.6 mCi. The data were acquired with and without a 20 cm diameter cylindrical water phantom in the tomograph using different masks. Data at the far right are for all mask bits set (no events rejected and therefore no masking). Notice the break in the horizontal axis.

The horizontal extent of the mask was varied in increments of 2 bins per angle resulting in 9 different masks with horizontal width varying from 4 to 20 bins (1.5% to 7.5% of mask bits set). The lateral distance between adjacent projection bins is 1.57 mm. The downward trend at the far left of figure 5 indicates

that the mask is cutting into the set of events for which the photons detected came from the same positron. We assume that these are good unscattered data, and we should therefore choose a mask with at least 3% of the mask bits set.

The masking does not have a dramatic effect on the effective data rate except for the 20.6 mCi source. For this source the effective data rate increases by a factor of 1.6, which is significant. Since accidental coincidences were the rate-limiting factor in transmission data acquisition, the new method allows us to acquire sufficient transmission data in a shorter time with a more active transmission source.

Acknowledgements

This work was supported in part by the Director, Office of Energy Research, Office of Health and Environmental Research of the U.S. Department of Energy, under Contract No. DE-AC03-76SF00098, and in part by Public Health Service Grant Nos. P01 HL25840 and R01 CA38086, awarded by the National Heart Lung and Blood and National Cancer Institutes, Department of Health and Human Services.

References

[1] M. E. Phelps, E. J. Hoffman, N. A. Mullani, and M. Ter-Pogossian. Application of annihilation coincidence detection to transaxial reconstrucion tomography. *J Nucl Med*, 16:210–224, 1975.

[2] S. E. Derenzo, T. F. Budinger, R. H. Huesman, J. L. Cahoon, and T. Vuletich. Imaging properties of a positron tomograph with 280 BGO crystals. *IEEE Trans Nucl Sci*, NS-28:81–89, 1981.

[3] L. R. Carroll, P. Kretz, and G. Orcutt. The orbiting rod source: Improving performance in PET transmission correction scans. In P. D. Esser, editor, *Emission Computed Tomography - Current Trends*, pages 235–247, Society of Nuclear Medicine, New York, 1983.

[4] C. J. Thompson, A. Dagher, D. N. Lunney, S. C. Strother, and A. C. Evans. A technique to reject scattered radiation in PET transmission scans. In O. Nalcioglu, Z. H. Cho, and T. F. Budinger, editors, *Proceedings of the International Workshop on Physics and Engineering of Computerized Multidimensional Imaging and Processing*, pages 244–253, SPIE 671, 1986.

[5] S. E. Derenzo, R. H. Huesman, J. L. Cahoon, A. Geyer, D. Uber, T. Vuletich, and T. F. Budinger. Initial results from the donner 600-crystal positron tomograph. *IEEE Trans Nucl Sci*, NS-34:321–325, 1987.

[6] P. Edholm. Tomogram reconstruction using an opticophotographic method. *Acta Radiologica Diagnosis*, 18:126–144, 1977.

[7] J L Cahoon, R H Huesman, S E Derenzo, A B Geyer, D C Uber, B T Turko, and T F Budinger. The electronics for the Donner 600-crystal positron tomograph. *IEEE Trans Nucl Sci*, 33(1):570–574, 1986.